Structural Unfreezing and Endothermic Effects in Liquids, β-D-Fructose

E. Tombari, G. Salvetti, and C. Ferrari

Istituto per i Processi Chimico-Fisici del CNR, via G. Moruzzi 1, 56124 Pisa, Italy

G. P. Johari*

Department of Materials Science and Engineering, McMaster University, Hamilton, Ontario L8S 4L7, Canada

Received: May 7, 2004; In Final Form: August 9, 2004

Both structural unfreezing and irreversible endothermic change between different molecular states of a material can occur on heating its liquid state and produce a double sigmoid-shaped endotherm in its apparent heat capacity, C_p. In such a case, the usual calorimetry is unable to distinguish between the molecular mechanisms of the two endothermic contributions. We report that this distinction can be made by measuring C_p and the complex heat capacity, C_p^*, simultaneously in a temperature-modulated scanning mode. When a sigmoid-shaped increase is observed in both C_p and C_p^* of a liquid, the underlying process is structural unfreezing. But, when this increase is observed in normal scanning and not in the temperature-modulated mode, the underlying process is either irreversible or too slow, compared to the modulation period. The method has been used for resolving the nature of tautomeric transformation in liquid β-D-fructose. Simultaneous C_p and C_p^* measurements show that, for normal scanning, C_p increases in a sigmoid-shaped manner with hysteresis, but for temperature-modulated scanning, the real component of C_p does not increase in this manner (i.e., the reversible component of the heat flow shows neither a sigmoid-shaped increase nor hysteresis). Therefore, the sigmoid-shaped C_p increase observed in normal scanning indicates an endothermic transformation in the β-D-fructose liquid at $T > T_g$ and not unfreezing of tautomeric transformation on the time scale of heating.

1. Introduction

In thermodynamics and molecular kinetics studies of a glass, structural unfreezing and enthalpy recovery are studied by measuring the slow rise in the time- and temperature-dependent heat flow or the apparent heat capacity, C_p.[1,2] This is done by using differential scanning calorimetry (DSC), which measures C_p as a glass is heated at a fixed rate.[1,2] Over a certain temperature range, the DSC scans show a sigmoid-shaped region with a slight overshoot in C_p, which makes this region resemble a broad endotherm. The details of the sigmoid-shaped C_p increase are determined by (i) the distribution of structural relaxation times and (ii) the sensitivity of the characteristic time to temperature. Increase in C_p in this manner is an indication of the recovery of the ergodic state on heating a (nonergodic) glass.[1,2] The onset temperature of the sigmoid-shaped C_p increase is taken as T_g, the glass softening (or glass transition) temperature. For the usual heating rate of 10 K/min in a DSC experiment, T_g is regarded as the temperature at which a glass softens to a viscosity of $10^{12}-10^{13}$ Poise.

Kinetic unfreezing of chemical reaction equilibrium on heating can also produce a sigmoid-shaped decrease in C_p. This is expressed in terms of a two-site model, which has been used to describe vitrification on cooling and glass softening on heating.[3,4] Accordingly, when the transition between the two states on cooling becomes slower than the decrease in T, the structure becomes kinetically frozen and the state becomes nonergodic, that is, the liquid vitrifies. (This is a general consequence of all phenomena described within a two-site model, including the point defects equilibrium.[5]) In terms of a chemical or physical equilibrium, the equilibrium constant, K, changes with T and freezes-in at a temperature where K in the liquid changes more slowly than its T. At a T below this freezing-in temperature, K is seen formally as Q, the reaction quotient, which approaches K spontaneously with time. Thus, the time- and temperature-dependent enthalpy change can be discussed in terms of Q.[6] Far-IR spectra of the freezing-in of a conformational equilibrium have been reviewed by Fishman et al.,[7] and a similar freezing-in is found during isothermal vitrification of a liquid by polymerization, whose C_p decreases with time in a sigmoid-shaped manner.[8a]

A sigmoid-shaped C_p increase may also appear on unfreezing of conformational equilibrium in a low-viscosity liquid. Because this feature has been associated with structural freezing (referred to as ergodicity breaking) on vitrification during cooling, it has been taken as conformational freezing (referred to as conformational ergodicity breaking). Kishimoto et al.[8b] have expressed such a conformational unfreezing of the $(Cl_2F)C-C(FCl_2)$ molecule, which they had observed in a plastic crystal state, in terms of the Schottky anomaly.

In general, a continuous transition of a low energy state to a higher energy state, without an equilibrium between the two states, can also produce a slow sigmoid-shaped C_p increase on heating. If the transition between the two states were to involve an additional transformation to a third state, the process may not completely reverse on cooling. Because adiabatic calorimetry and DSC are rarely performed by cooling a liquid, the mechanism for the sigmoid-shaped C_p increase may not be resolved by these techniques. As interest in thermodynamic and kinetic studies of supercooled liquids rapidly grows, there is a need to develop criteria and procedures by which the mechanisms for endothermic features may be distinguished. Here, we describe such a procedure by using simultaneous measurements

10.1021/jp048036r CCC: $27.50
Published on Web 10/06/2004

of the apparent heat capacity, C_p, and complex heat capacity, C_p^*, by using temperature-modulated scanning calorimetry (TMSC). As an example, we use a low-viscosity melt of β-D-fructose. The sugar itself exists in tautomeric forms, and its melt does not crystallize on cooling. The study leads to an understanding of both the transformation kinetics and thermodynamics in the liquid state and helps in resolving the mechanism behind the sigmoid-shaped C_p increase observed in DSC studies.

2. Experimental Methods

β-D-fructose of 99+% purity was purchased from Aldrich Chemicals and used as such. The modulated adiabatic and scanning calorimeter used for the study has been described elsewhere.[9] Although this calorimeter can be used for measurements in both adiabatic and temperature scanning methods, it was used only in the temperature scanning mode of both heating and cooling. The C_p and C_p^* of the sample were measured simultaneously by using TMSC technique, in which the temperature is programmed as a temperature ramp at fixed average rate of heating or cooling on which a sinusoidal modulation of 0.5 K amplitude and 3.3 mHz frequency was superimposed. The instrument was calibrated by using dodecane and glycerol as standard liquids for heat capacity, and absolute heat capacity values were obtained. Measurements were repeated with different samples, and the reproducibility of the data was found to be better than 1%.

In a typical experiment, β-D-fructose crystals were transferred into a ~2-mm internal diameter glass sample holder closed at one end, and their mass was accurately determined. The sample holder was then hermetically sealed by melting its open end in a narrow flame. It was then transferred to the sample cell of the calorimeter, which had been isothermally kept at 383.2 K. While inside the calorimetric assembly at 383.2 K, the sample's melting was observed for 3.1 h. The temperature profile of the sample and the plot of the rate of heat absorbed in the melting process against time are shown in Figure 1A. (Note that the sharp minimum in temperature of the sample occurred at the instant of introducing the sample into the calorimeter.) The liquid sample was thereafter quenched to 247 K, kept at that temperature for 2 ks (=0.55 h), and then heated from 247 to 373 K at 24 K/h rate. It was kept at 373 K for 7.2 ks and then cooled back to 247 K at 24 K/h, kept for 2 ks at 247 K, and the process repeated. The temperature−time profile for these experiments, to which the modulation is added, is provided in Figure 1B. Here, the sloping lines 1−7 represent the average heating and cooling, and horizontal lines represent the (temperature-modulated) quasi-isothermal conditions.

3. Criteria for Distinguishing Endothermic Features

Because most thermodynamic studies of glasses have been performed by using the DSC technique, the basis of this technique is generally known in this area. But because C_p and C_p^* measurements by the TMSC technique are relatively new and unfamiliar, we will describe this briefly here. We will also describe (i) how the information obtained from DSC and TMSC differs, (ii) how the various contributions to the C_p are determined from TMSC, and (iii) how the difference between C_p and C_p^* data will be used here to deduce information on the irreversible and reversible thermodynamic changes. It should be noted that the modulation frequency used in our TMSC technique is necessarily low. Therefore, the heating and cooling rates for scanning in a TMSC experiment have to be considerably lower than those for DSC, so that the time scale for

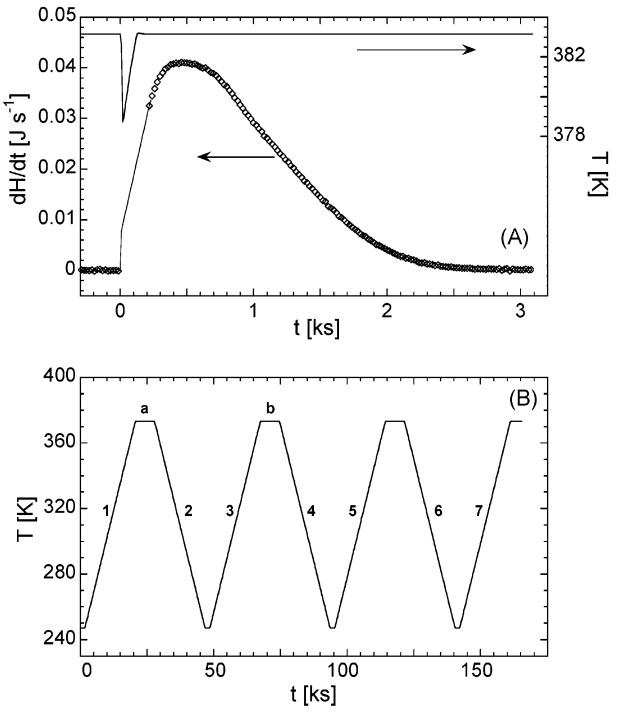

Figure 1. (part A) Temperature profile used for heating β-D-fructose and the heat flow needed during its melting. (part B) Temperature−time profile used in the experiment and to which temperature modulation was added. The heating and cooling rates are 24 K/h (0.4 K/min); the modulation amplitude is 0.5 K and the modulation frequency 3.3 mHz (modulation cycle of 300 s).

structural freezing and unfreezing can be determined by this (cooling and heating) rate rather than by the temperature modulation rate. This places a limit on the modulation frequency range that can be used in TMSC. Hence, measurements are usually performed for a single frequency. For further details, the reader may consult refs 10 and 11.

In the temperature-modulated technique, TMSC, the rate of only that part of the heat stored or released which reverses with reversal of the temperature is measured. The components of the complex heat capacity, C_p^*, oscillating in phase with the temperature, C_p', and oscillating out of phase, C_p'', are calculated during the course of the temperature modulation cycle. The two components are related to the modulation amplitude and the modulation period, $t_{mod} = 2\pi/\omega$, where ω is the angular frequency of temperature modulation (for details, see ref 9).

In DSC, the rate of heat flow is measured. From that rate, the heat capacity, $C_{p,DSC}$, is calculated from the equation

$$C_{p,DSC} = \left(\frac{1}{\beta}\right)\left(\frac{dH(T,t,x_A)}{dt}\right) \quad (1)$$

where $[dH(T,t,x_A)/dt]$ is the measured rate of enthalpy change and β (=dT/dt) is the temperature scanning (heating or cooling) rate. Equation 1 can be written in a more general form by taking into account the two time-dependent quantities, (i) the temperature T and (ii) the mole fraction x_A of the entity A undergoing a chemical change to, for example, entity B. Therefore, for C_p measured in a DSC experiment

$$C_{p,DSC} = \left[C_{p,thermo} + \left(\frac{\partial H}{\partial x_A(T)}\right)\left(\frac{dx_A}{dT}\right)\right] + \left(\frac{1}{\beta}\right)\left[\frac{\partial H}{\partial t} + \left(\frac{\partial H}{\partial x_A(t)}\right)\left(\frac{dx_A}{dt}\right)\right] \quad (2)$$

where $C_{p,thermo} = \partial H/\partial T$ is the thermodynamic or true heat capacity. For this case, the term $[(\partial H/\partial x_A)(dx_A/dT)]$ in eq 2 refers to a thermally reversible transformation process of entity A to entity B, which may be fast enough that equilibrium is maintained at every instant of the temperature modulation period, and consequently, the original state of the system would be restored after one modulation cycle.

Comparison of the data obtained from the DSC and TMSC techniques is simpler when $C_p'' = 0$, because for such a condition, the magnitude of C_p' is given by the first term in the square brackets in the right-hand side of eq 2. Hence,

$$C_{p,DSC} = C_p' + \left(\frac{1}{\beta}\right)\left[\frac{\partial H}{\partial t} + \left(\frac{\partial H}{\partial x_A(t)}\right)\left(\frac{dx_A}{dt}\right)\right] \qquad (3)$$

From eq 2, we identify three conditions for the occurrence of a chemical and/or physical process in terms of the enthalpy change as follows:

(i) When $(\partial H/\partial x_A) = 0$, or when $(dx_A/dT) = 0$, and the quantities $(dx_A/dt) = 0$ and $(\partial H/\partial t) = 0$ (i.e., there is neither a chemical nor a physical process for producing a temperature- and time-dependent change in the enthalpy). In this case, the measured value of C_p from a DSC experiment is given by

$$C_{p,DSC} = C_{p,thermo} = C_p' \qquad (4)$$

(ii) When $(\partial H/\partial x_A) \neq 0$, $(dx_A/dT) \neq 0$, but $(\partial H/\partial t) = 0$ and $(dx_A/dt) = 0$ (i.e., there is a fast reversible (chemical or physical) process that restores the original state of the sample at any time within the time period of the temperature modulation cycle, and there is no irreversible (physical or chemical) process). Therefore, the last term in the square brackets in eq 2 is zero. In this case, the measured value is given by

$$C_{p,DSC} = \left[C_{p,thermo} + \left(\frac{\partial H}{\partial x_A(T)}\right)\left(\frac{dx_A}{dT}\right)\right] = C_p' \qquad (5)$$

In expressing $(dx_A/dt) = 0$ in eq 5, an equilibrium between two states, A and B, may coexist, and the time required for the equilibrium is much faster than the modulation period, with the result that during the modulation an equilibrium between A and B is maintained. The equilibrium constant of the A $\leftrightarrow$ B is temperature dependent, as is implicit in $(dx_A/dT) \neq 0$.

(iii) When $(\partial H/\partial x_A) \neq 0$, $(dx_A/dT) \neq 0$, $(\partial H/\partial t) \neq 0$, and $(dx_A/dt) \neq 0$ (i.e., there are slow and irreversible (chemical or physical) processes that continue to occur with time at that T; that is, the rate of these processes is slow enough that the original state is not restored during the modulation cycle, and there is also a time-dependent enthalpy arising from an irreversible (chemical or physical) process). In this case

$$C_{p,DSC} \neq C_p' \qquad (6)$$

Because the quantities $C_{p,DSC}$ and C_p' may be simultaneously determined in our experiments, we use the previously given relationships between them as a basis for our discussion and, further, as a criteria for identifying the nature of the endothermic process. For conditions (i) and (ii), the TMSC and DSC experiments yield the same C_p value, but for condition (iii), they do not. Therefore, when a physical or chemical process is reversible, and the characteristic time for the transformation is much less than the temperature modulation period, the measured C_p values in the TMSC and DSC experiments would be identical. In cases when the physical or chemical process is irreversible and/or slow (i.e., $(\partial H/\partial t) \neq 0$ and/or $(dx_A/dT) \neq 0$) the data obtained by TMSC do not show the same features as the DSC data, and the TMSC data do not contain the effects of irreversible enthalpy changes. In general, when $C_{p,DSC}$ in the simultaneous measurements, as performed here, shows an endothermic increase and C_p' does not, the endothermic increase observed in $C_{p,DSC}$ is due to an irreversible effect, not to structural unfreezing on the time scale of the heating scan.

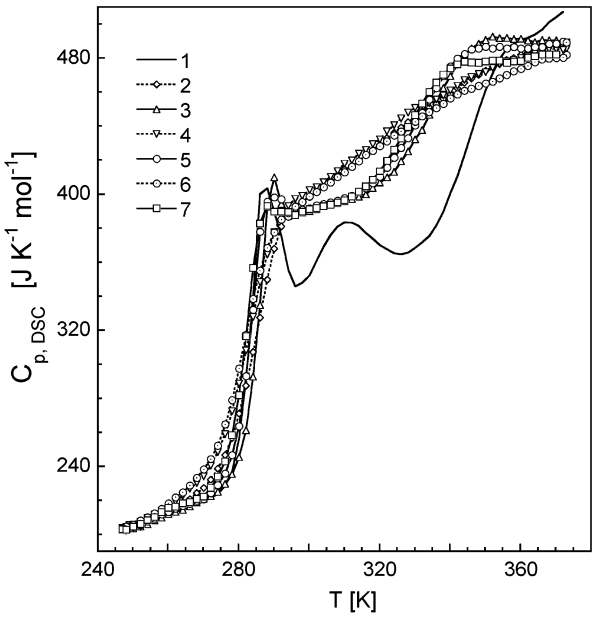

Figure 2. Apparent heat capacity of β-D-fructose, or $C_{p,DSC}$, is plotted against the temperature. Numbering of the curves corresponds to the heating and cooling profiles as in Figure 1B. Curves 1, 3, 5, and 7 are for measurements made during heating, and curves 2, 4, and 6 are for those made during cooling. The heating and cooling average rates are 24 K/h.

4. Results and Discussion

A. Apparent Heat Capacity from Scanning Calorimetry or DSC. The C_p values derived from the single period average of the heat flow measured by TMSC, equivalent to those derived by DSC,[10] are plotted against the temperature in Figure 2. Here, curves 1, 3, 5, and 7 are from the measurements made during heating, and curves 2, 4, and 6 from those made during cooling, as in the procedure shown in Figure 1B. In these plots, the sharp, sigmoid-shaped increase in $C_{p,DSC}$ with an onset at 270−280 K is the usual glass-softening endotherm, which is attributable to the beginning of the ergodicity recovery. At $T < 270$ K, the enthalpy has been found to decrease with time, a behavior characteristic of the glassy state,[1,2] as is the decrease in the heat capacity.[12] At $T > 290$ K, which is much higher than its glass-softening temperature, T_g, of 275−280 K, the state is fluid, and therefore, it is expected to be in an apparent internal equilibrium. Nevertheless, the fluid state at $T > 290$ K also shows a broad, sigmoid-shaped increase in $C_{p,DSC}$ in Figure 2.

The sharp, sigmoid-shaped $C_{p,DSC}$ increase observed over the glass-softening temperature range of 247−290 K in the seven plots in Figure 2 is qualitatively similar, but subtle differences remain. For example, a scrutiny of curves 1, 3, 5, and 7 shows that $C_{p,DSC}$ measured at the same temperature during heating at the same rate differs, as does $C_{p,DSC}$ measured during cooling in curves 2, 4, and 6. These differences are likely to arise from the change in concentration of the fructose molecule's isomeric species in the liquid on thermal cycling and/or a slight decomposition of fructose that alters its overall viscosity and distribution of relaxation times and, hence, changes the shape

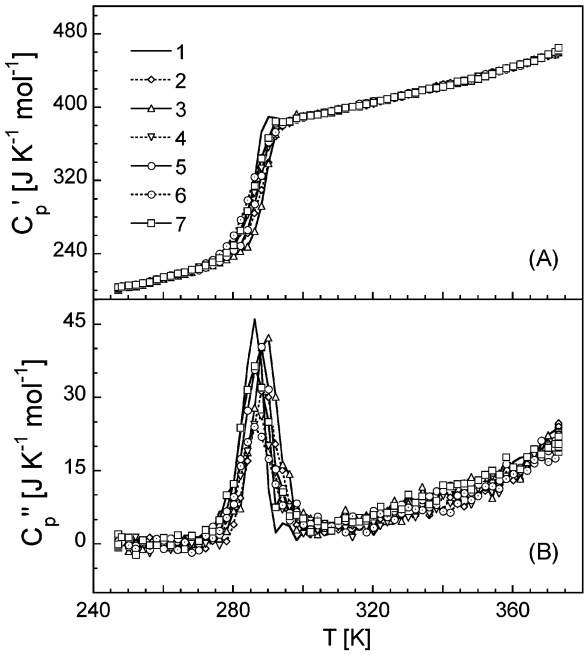

Figure 3. (part A) The real component of C_p^* (i.e., C_p') of β-D-fructose measured in the temperature-modulated experiment is plotted against the temperature. (part B) The imaginary component of C_p^* (i.e., C_p') is plotted against the temperature. The data refer to the same conditions as for part A. Numbering of the curves corresponds to the heating and cooling profiles as in Figure 1B. Curves 1, 3, 5, and 7 are for measurements made during heating, and curves 2, 4, and 6 for those made during cooling. The heating and cooling average rates are 24 K/h.

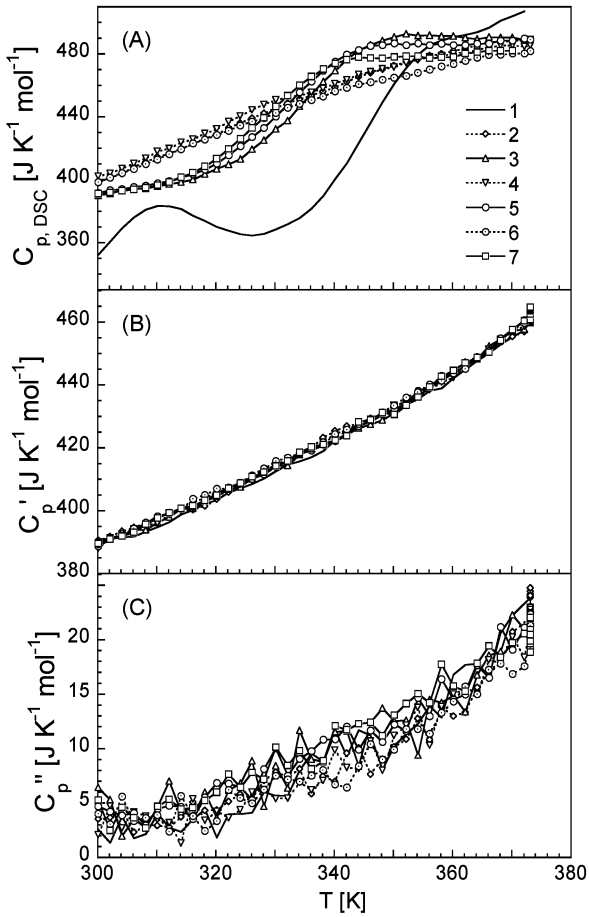

Figure 4. (part A) The apparent C_p, or $C_{p,DSC}$, of liquid β-D-fructose is plotted against the temperature. (part B) Corresponding plots of the real component of C_p^* (i.e., C_p'). (part C) Corresponding plots of the imaginary component of C_p^* (i.e., C_p'). Numbering of the curves corresponds to the heating and cooling profiles as in Figure 1B, and data are shown only at $T > 290$ K. Curves 1, 3, 5, and 7 are for measurements made during heating, and curves 2, 4, and 6 are for those made during cooling. The heating and cooling average rates are 24 K/h.

of the curves in the glass-softening range. Curve 1 in Figure 2, which is for the sample that had been quenched from 383.4 to 247 K, kept at that temperature for 2 ks, and thereafter heated, shows a small $C_{p,DSC}$ overshoot in the 285−290 K range, followed by a local minimum in $C_{p,DSC}$ at 297 K. Because the $C_{p,DSC}$ value at the minimum is less than the value observed in all subsequent curves, the minimum indicates an exothermic transformation in the liquid β-D-fructose. This aspect will be discussed later.

B. Complex Heat Capacity from Temperature-Modulated Calorimetry. From the data measured by using TMSC, the real (in-phase component), C_p', of the complex heat capacity, C_p^* and the imaginary (out-of-phase) component, C_p'', were calculated from the equation $C_p^* = C'_p - iC_p''$, where $i = (-1)^{1/2}$. The C_p' and C_p'' values are plotted against the temperature in Figure 3A and 3B, respectively. Here also, curves 1, 3, 5, and 7 are from measurements made during heating, and curves 2, 4, and 6 are from those made during cooling. Here also, the sigmoid-shaped C_p' increase in all seven curves is remarkably similar over the glass-softening range of 247−290 K, but differences remain in the values obtained for different plots. At temperatures higher than 290 K, the C_p' values measured in different experiments from 1−7 are identical, and the values measured during heating and cooling retrace the same curve.

Figure 3B shows that, over the temperature range of 247−290 K, a peak appears in the plots of C_p'' and the position and height of this peak differs in different plots. At temperatures above 290 K, there is a gradual increase in C_p'' with an increase in temperature, but the C_p'' values in the measurements performed during heating and cooling still lie within the expected range of scatter of ∼2%. This increase is a result of continuation of the reversible slow process which raises both C_p' and C_p'', as we will discuss in the next section.

C. Comparison of the Temperature-Modulated and Unmodulated Studies. Over the temperature range of 247−290 K, the $C_{p,DSC}$ data in Figure 2 differ from the C_p' data in Figure 3A, whether measured during heating or during cooling. Peaks, minima, or sigmoid-shaped rises in C_p , which appear in the plots of $C_{p,DSC}$, do not appear in the plots of C_p'. Part of the difference is clearly due to the (irreversible) enthalpy relaxation, which contributes to the $C_{p,DSC}$ but not to the C_p'. Because our interest here is in the study of the low-viscosity state of β-D-fructose as an example of liquids whose molecules undergo conformational changes, we will discuss only the C_p features observed at $T > 290$ K. The $C_{p,DSC}$ and C_p' data at $T < 290$ K and a detailed analysis of the structural relaxation of β-D-fructose in the glass-softening range will be reported in the future, along with a comparative discussion with other materials.

To examine the $C_{p,DSC}$ and C_p' features of liquid β-D-fructose, we replot in Figure 4 A the $C_{p,DSC}$ measured during heating from 300−373 K and cooling back down to 300 K. Curve 1, which is for the sample melted at 383.2 K, quenched to 247 K, kept for 2 ks at 247 K, and finally heated to 373.2 K, shows an exothermic minima at 328 K, which is in addition to the minimum at 297 K already seen in Figure 2. The two minima, one at 297 K (Figure 2) and the other at 328 K (Figure 4A) indicate two consecutive exothermic transformations. The

plot further shows that the state formed in the first exothermic transformation converts to another state in the second exothermic transformation. This is supported by the observation here that neither of these two exotherms appears in subsequent $C_{p,DSC}$ data, as is shown by curves 3, 5, and 7 in Figure 2.

In Figure 4A, curve 3 shows a broad, sigmoid-shaped increase in $C_{p,DSC}$ with onset at approximately 320 K and ending at 340−350 K, indicating that heat is being continuously absorbed in the liquid by a relatively slow process. Curves 5 and 7, obtained during cooling of the melt and subsequent heating, both show that the height of the stretched, sigmoid-shaped $C_{p,DSC}$ rises and its onset temperature decreases. The decrease in the height indicates a continuous decrease in the endothermic effect in these subsequent cycles. Remarkably, the $C_{p,DSC}$ plots measured during cooling do not show a pronounced sigmoid-shaped curve of the type seen in curves 1, 3, 5, and 7 in Figure 4A. Instead, they show an almost smooth return to the original $C_{p,DSC}$ value at $T < 300$ K. Curves 2, 4, and 6 in Figure 4A show that the onset temperature of the broadened decrease in $C_{p,DSC}$ measured during cooling is even lower than the end temperature of the sigmoid-shaped increase in the $C_{p,DSC}$ of curves 1, 3, 5, and 7 measured during heating. This is the opposite of what has been observed for the glass-softening endotherms shown in Figure 2, where the onset temperature of the $C_{p,DSC}$ decrease in measurements made during cooling (curves 2, 4, and 6) is higher than the end temperature of the $C_{p,DSC}$ increase in measurements made during heating (curves 1, 3, 5, and 7). In addition, the 5−7 K range for the glass-softening endotherm seen in Figure 2 is much less than the 35−40 K range of the sigmoid-shaped curve in Figure 4A.

The C_p' values for the corresponding heating and cooling are plotted in Figure 4B, and the C_p'' values are plotted in Figure 4C. It is evident that no sigmoid-shaped increase in C_p' occurs, and there is no peak in C_p''. All data for the seven curves in Figure 4B clearly lie on a single curve of C_p'. Similarly, the data in Figure 4C lie on a single curve of C_p'', within the scatter of the data.

On heating from 320 to 380 K, there is a gradual, nonlinear increase in C_p', and $C_p'' \neq 0$. These arise from a slow occurrence of a partially reversible chemical or physical process. This aspect will be discussed in detail in the future by comparing these results against those predicted by a two-state equilibrium model.

We conclude that the true (thermodynamic) heat capacity of β-D-fructose liquid is approximately given by the data points in the C_p' plots in the sets of curves in Figure 4B, which is the same whether measurements are made on heating or on cooling. The C_p' deviations from nonlinearity and the C_p'' values reach the maximum of ∼2% of the measured thermodynamic heat capacity.

The absence of a sigmoid-shaped C_p' rise, as well as the absence of a peak in C_p'' in Figure 4A and B, show that the chemical and/or physical processes, which produce the sigmoid-shaped increase in $C_{p,DSC}$ in Figure 4A, do not cause thermodynamic heat capacity changes, which should contribute to C_p^*. Thus, any tautomer equilibrium change occurring at a certain rate is either not reversed in the sinusoidal modulation cycle or is reversed, but the rate of reversal is much slower in comparison with the modulation frequency. Alternatively stated, any endothermic transformation that produces a sigmoid-shaped rise in $C_{p,DSC}$ of β-D-fructose is a consequence of an irreversible or slow process that has no effect on the thermodynamic heat capacity observed by TMSC. Therefore, if the sigmoid-shaped $C_{p,DSC}$ increase observed on heating liquid β-D-fructose with an onset temperature of ∼315 K was due to the unfreezing of

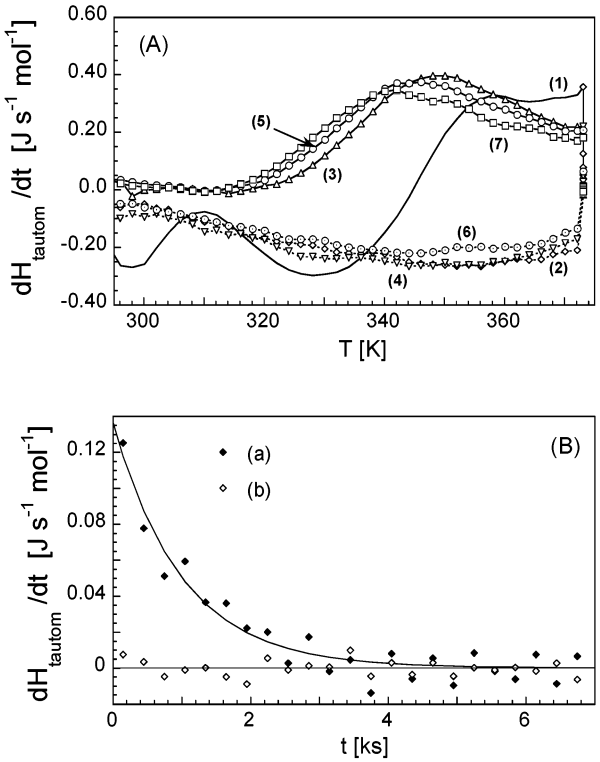

Figure 5. (part A) Rate of heat evolved by the slow and/or irreversible tautomeric transformation between different states of liquid β-D-fructose, or dH_{tautom}/dt, is plotted against the temperature. Labeling of the curves refers to the conditions given in Figure 1B. (part B) Rate of heat evolved plotted against time when β-D-fructose was kept isothermally at 373 K after the first heating in region a of the plot in Figure 1B and after the second heating in region b.

tautomerization equilibrium, generating a change in thermodynamic heat capacity, TMSC experiments would show a sigmoid-shaped rise in C_p' in the same manner as has been observed during vitrification of β-D-fructose on cooling and during glass softening on heating in Figure 2. But, our TMSC experiments do not show this.

To investigate the origin of the high temperature $C_{p,DSC}$ features, we determine from eq 3

$$\frac{dH_{tautom}}{dt} = \frac{\partial H}{\partial t} + \left(\frac{\partial H}{\partial x_A(t)}\right)\left(\frac{dx_A}{dt}\right) = (C_{p,DSC} - C_p')\frac{dT}{dt} \quad (7)$$

where dH_{tautom}/dt takes into account the rate of enthalpy changes due to the slow and/or irreversible tautomeric transformation between different states. Positive values of dH_{tautom}/dt indicate endothermic transformations from one state to the other; negative values indicate exothermic, partially reversing processes.

The quantity dH_{tautom}/dt is plotted against T in Figure 5A, where the curves 1−7 are labeled as in Figure 1B. Curve 1 shows that dH_{tautom}/dt is negative beginning at 290 K and ending at ∼345 K, and the total curve appears to be composed of two minima, one ending near 310 K and the other ending at 330 K. In curve 2, which is for subsequent cooling, the negative dH_{tautom}/dt shows a minimum at $T = 355$ K. On subsequent heating shown by curve 3, dH_{tautom}/dt is zero or negligible in the 290−315 K range, and then, it increases approximately toward the same value as for curve 1. Subsequent thermal cycling decreases dH_{tautom}/dt in the high-temperature limit, which means that the enthalpy of β-D-fructose at high temperatures decreases on further thermal cycling. Because dT/dt is the same

in all measurements, these plots show that the height and the area under the ($C_{p,DSC} - C'_p$) plot decreases, as does its value at 373 K, the highest measurement temperature. This is another manner of showing that an irreversible chemical and/or physical change also occurs on thermal cycling of β-D-fructose.

These features indicate that there are two exothermic processes of tautomerization in the quenched β-D-fructose liquid (curve 1 in Figures 2A, 4A, and 5A) and the heat evolved in these processes is considerably reduced on thermal cycling, as expressed by curves 1, 2, and 3, and is further reduced by thermal cycling, as expressed by curves 3, 5, and 7 in Figure 5A. Thus, the products formed by the first exothermic processes on heating the quenched β-D-fructose melt (curve 1) seem to convert to another product by another exothermic process. Because these results differ fundamentally from the DSC data on which an earlier interpretation had been based (readers may consult the original paper in ref 13), a new interpretation of the results is needed, as follows.

In our earlier dielectric study of liquid β-D-fructose,[14] we had reviewed the various conformational states that exist in the liquid and crystalline states of β-D-fructose. We use that as a basis here. Briefly, at a molecular level, the state of the liquid obtained by quenching after keeping for 3.1 h at 383.2 K in our interpretation contains less β-pyranose and more of both α- and β-furanose than their equilibrium values at 290 K. (Note that crystalline β-D-fructose contains 100% β-pyranose, which is also the lowest energy conformational state.) On the first heating of the quenched liquid, β-pyranose forms exothermally. Because the time taken in thermal cycling (9 h in the heating plus cooling over the 84 K range, the temperature interval of this study in which the sample is in the liquid state) is longer than the time taken in the earlier study[13] (8.4 min), only a small fraction of the excess amounts of other components persist at 290 K after the first thermal cycle. The endothermic part of the curves at $T > 345$ K, would then represent the formation of species of higher energies. Because these species are of different internal energies, different amount of energies would be absorbed, depending upon their concentrations.

Finally, the heat released when β-D-fructose was kept at a fixed temperature of 373 K is plotted against time in Figure 5B. In it, curve a corresponds to the isothermal condition of the horizontal curve a in Figure 1B (i.e., after the quenched sample had been heated to 373 K), and curve b corresponds to the isothermal condition of the horizontal segment b in Figure 1B after the second heating of the same sample. In the first case, heat is released, and the rate of heat flow approaches zero with a time constant of about 1.5 ks and an amplitude, extrapolated to $t = 0$ of the isotherm, of 0.13 J s^{-1} mol^{-1}. On the contrary, in the second case, no detectable heat flow occurs (i.e., the dH_{tautom}/dt decays to a value of zero in a time on the order of the modulation period, when the heating ramp is finished). Therefore after the second heating, the molecular states in the β-D-fructose liquid undergo no further change.

It should be noted that, despite the fact that neither a sigmoid-shaped increase in C'_p nor a peak in C'_p has been observed for the melt at $T > 300$ K, and therefore, the purpose of this study has been fulfilled, it would still seem desirable to perform multifrequency measurements or, alternatively, obtain a spectra so that some idea of the relaxation time could be obtained by analyzing part of the spectra. But, doing so requires new equipment, particularly when the frequencies required for measurements must differ by at least an order of magnitude so that effects could be resolved in a temperature plane. We plan to develop such equipment in the future.

5. Conclusions

Simultaneous measurements by temperature-modulated scanning calorimetry of a model liquid β-D-fructose show that the endothermic effect seen as a broad, sigmoid-shaped increase in C_p is an indication of a slow endothermic conversion of the tautomeric states on heating and a slow exothermic conversion on cooling. This conversion is not significantly reversed within a temperature modulation cycle of 300 s, and therefore, the C_p's measured by the two techniques differ. There is no indication of enthalpy or entropy freezing on cooling (or unfreezing on heating) β-D-fructose over a temperature range (above its T_g) when it remains a liquid. Therefore, no evidence for freezing-in of the tautomeric equilibrium has been found here. We propose that similar studies by normal scanning and temperature-modulated scanning performed simultaneously on the same sample would be helpful, not only for understanding the nature of kinetic and thermodynamic transitions in liquids, but also for determining whether a liquid exists in a metastable state, like that of a glass, after a conformational equilibrium of its molecules becomes kinetically frozen-in at the time scale of its cooling. We suggest that such studies of liquids would be useful in resolving the thermodynamic effects of molecular conformational changes from those of the overall structural changes.

Acknowledgment. G.P.J. would like to thank IPCF-Sede, CNR, Pisa, for their hospitality during his stay for the duration of this study and the Natural Sciences and Engineering Research Council of Canada for a Discovery Research Grant for support of his general research.

References and Notes

(1) For a review, see Hodge, I. M. *J. Non-Cryst. Solids* **1994**, *169*, 211.
(2) Scherrer, W. G. *Relaxation in Glass and Composites*; Wiley: New York, 1986.
(3) Macedo, P. B.; Capps, W.; Litovitz, T. A. *J. Chem. Phys.* **1966**, *44*, 3357.
(4) Angell, C. A.; Rao, R. J. *J. Chem. Phys*. **1972**, *57*, 470.
(5) Perez, J. *Physique et Mechanique des Polymeres Amorphes* (English Translation by Balkama, A. A., 1998); Tec & Doc: Paris, 1992.
(6) Johari, G. P.; Sartor, G. *J. Phys. Chem.* **1997**, *101*, 8331.
(7) Fishman, A. I.; Stolov, A. A.; Remizov, A. B. *Spectrochim. Acta, Part A* **1993**, *49*, 1435.
(8) (a) Ferrari, C.; Salvetti, G.; Tombari, E.; Johari, G. P. *Phys. Rev. E* **1996**, *54*, R1058. (b) Kishimoto, K.; Suga, H.; Seki, S.; *Bull. Chem. Soc. Jpn.* **1978**, *51*, 1691.
(9) Salvetti, G.; Tombari, E.; Mikheeva, L.; Johari, G. P. *J. Phys. Chem. B* **2002**, *106*, 6081.
(10) See papers in special issue of *Thermochim. Acta* **1995**, *304*−*305*.
(11) Schawe, J. *Thermochim. Acta* **1995**, *260*, 1; **1995**, *261*, 183.
(12) Tombari. E.; Salvetti, G.; Johari, G. P. *J. Chem. Phys.* **2002**, *117*, 8436.
(13) Fan, J.; Angell, C. A. *Thermochim. Acta* **1995**, *266*, 9.
(14) Tombari, E.; Cardelli, C.; Salvetti, G.; Johari, G. P. *J. Mol. Struct.* **2001**, *559*, 245. In the abstract, "at 383 K" should read "at 283 K".